

## **An Experimental Study of Coal Dust Ignition in Wedge Shaped Hot Plate Configurations**

Kulbhushan A. Joshi

Graduate Student

Department of Fire Protection Engineering

Worcester Polytechnic Institute, Worcester, MA 01609

Vasudevan Raghavan

Assistant Professor

Department of Mechanical Engineering

Indian Institute of Technology Madras, Chennai, India 600036

Ali S. Rangwala

Assistant Professor and Corresponding Author

Department of Fire Protection Engineering

Worcester Polytechnic Institute, Worcester, MA 01609

Email: [rangwala@wpi.edu](mailto:rangwala@wpi.edu)

Phone: 508 831 6409

Fax: 508 831 5862

## **Abstract**

Ignition behavior of bituminous coal dust deposited between two hot surfaces forming wedges of 60°, and 90° is experimentally studied. Three thermocouples placed along the symmetry plane of the wedge cross-section at various heights from the apex (lowermost, middle and top) are used to record the transient temperature data. Results show that the ignition always occurs around the region surrounding the top thermocouple in the case of 60° wedge and both the top and the middle regions in the case of 90° wedge. The trends are explained by investigating three parameters affecting the ignition behavior, namely, the heat transfer from the hot plate to the coal dust, the subsequent chemical heat release, and the heat transfer between different regions within the coal dust. Furthermore, an experimental setup, similar to the standard ASTM E 2021 test, is used to determine the minimum ignition temperatures of coal layers of various thicknesses and to assess the ignition scenario in the wedge configuration using an effective length scale. Measured quantities such as minimum hot plate temperature that causes ignition and the ignition time, as well as the transient heat release rate and heat conducted between various zones, calculated based on the temperature data are used to quantify the three parameters and their effects on ignition behavior.

## **Keywords**

Thermal ignition; wedge geometry; coal dust; critical volume; minimum ignition temperature

## **Nomenclature**

$\alpha$	Angle between two hot surfaces
$\rho$	Bulk density (kg/m <sup>3</sup> )
A	Pre-exponential constant (1/s)
$A_c$	Area of cross section (m <sup>2</sup> )
c	Heat capacity of coal dust (J/kgK)
E	Activation energy (J/mol)
k	Bulk thermal conductivity (W/m-K)
n	dimensional $\theta$ -coordinate (m)
Q	Heat of reaction (J/kg)
r	radial coordinate (m)
$R_u$	Universal gas constant (J/mol-K)
$t_{ig}$	Time of ignition (minutes)
T	Instantaneous temperature (°C or K)
$T_p$	Hot plate temperature (°C or K)
$\theta$	angular coordinate (radians)

## 1. Introduction

Combustible dust layers can be ignited by a surface whose temperature is sufficiently high and the resulting fires after ignition can cause large losses in lives and property. In some cases these processes are the first step towards an escalating chain of events that can lead to both gas and dust explosions. Numerous case histories demonstrating such chain of events can be found in literature [1- 4]. The National Academy of Sciences (NAS) Committee on Evaluation of Industrial Hazards has recommended a hot surface test to determine minimum hot-surface ignition temperatures of dust layers. The International Electrotechnical Commission (IEC) has proposed a very similar test. These two test reports and the work by the US Bureau of Mines [5] generated the ASTM standard E 2021 [6] and the European standard EN 50281-2-1(1999) [7]. These tests are based on determining a reference minimum temperature necessary for the ignition of a dust. This is normally performed by exposing a sample, with standard dimensions and boundary conditions, to a fixed ambient temperature and observing whether ignition occurs. Common criteria for ignition in hot surface tests are visible signs of combustion or glowing, or the sample temperature rising to 50 °C above the hot surface temperature (ASTM E 2021). Experimental work on surface ignition of dusts using these test methods are published in literature and include different dust samples such as wood, metal, and coal tested at varying layer thicknesses from 5mm to 50mm [5, 8 - 12]. Among these studies, experimental studies by Bowes and Townshend [8], Reddy *et al.* [9], and Park *et al.* [10] have applied thermal ignition theory (Thomas and Bowes [13]) towards obtaining thermo-kinetic parameters that govern self-heating of the dust.

The minimum ignition temperature obtained from the above standard tests, however, cannot be applied to different geometries. In most industrial accidents, dust layer ignition usually initiates in corners and wedges where the dust is trapped. In addition, dust accumulation on a level surface can be easily cleaned, but the dust deposits in corners and grooves are typically left behind. The current test standards cannot address these issues where dusts accumulate in complex geometries. This is because modeling ignition for other geometries found in industrial environments is not possible solely from the measured ignition temperature at a specific dust layer thickness. Studies have shown that the ignition temperature is highly geometry dependent [14], and is therefore not a quantifiable parameter to analyze the risk associated with dust layers. The purpose of this study is to analyze the ignition behavior of a dust deposit trapped in a wedge shaped configuration having hot surfaces. Experiments with two hot plates, configured at two different angles (90° and 60°) to form wedges, have been carried out and the two-dimensional heat transfer effects are envisaged.

## 2. Experimental Setup

The experimental setup comprised of two stainless steel plates that were used as hot surfaces attached to each other to form a wedge like geometry as shown in Fig. 1. The angle of the wedge was adjusted by using a stainless steel base-plate (shaded light gray) which allowed the plates to be adjusted to an acute angle of  $60^\circ$  and a right angle of  $90^\circ$ . Each plate was attached to an electrically heated plate, ROPH-144, Omega engineering, with thermally conductive cement (Omegabond 700), to provide uniform temperature distribution all along the plate. The perimeter wall was also wrapped by a 5 mm thick insulating material (ceramic paper 390 manufactured by Cotronic Co.) to minimize the heat loss to the environment. The temperature of the plates was measured by a Type K surface temperature thermocouple, CO1-K, Omega engineering, 35 mm inside from the plate edge. Furthermore, experiments with a flat hot plate, equivalent to a  $180^\circ$  wedge, were conducted using a setup similar to that reported by Park *et al.* [10]. This setup is comprised of a circular disc shaped hot plate (203 mm diameter) and uses stainless steel rings of different thicknesses to contain the coal dust layer.

A temperature controller, CN 8592, Omega engineering, and solid state relay, SSRL240DC25, Omega engineering, were used to control and maintain the hot surface temperature at a steady value throughout any given test. Temperatures on the stainless steel wedge set at  $250^\circ\text{C}$  showed very good uniformity. Temperatures were measured at 12 points on the hot surface, uniformly spaced, 6 points each and on two lines normal to each other. Except one point at which temperature was  $249^\circ\text{C}$ , the other 11 points reported  $250^\circ\text{C}$ . The thermocouples for both surface and dust layer temperature have an error of  $\pm 1.1^\circ\text{C}$  and the temperature controller, CN8592, has an error range of  $\pm 1^\circ\text{C}$  prescribed by the manufacturer. NI data acquisition unit has shown  $\pm 1^\circ\text{C}$  temperature fluctuation throughout tests. The inherent uncertainty of the test apparatus is within an acceptable range since tests were conducted with either 5 or  $10^\circ\text{C}$  resolution with respect to the layer ignition temperature. All tests were performed in a fume hood where ambient temperature was maintained at  $22^\circ\text{C}$ .

All tests were performed using Pittsburgh seam coal dust provided by CONSOL energy laboratory and reported to have an average particle size of  $32\ \mu\text{m}$ . The measured average bulk density was  $580\text{kg}/\text{m}^3$ . Other physical and chemical properties of the dust are reported in Park *et al.* [10]. The experimental procedure comprised of turning the hot plate on and using the temperature controller to set the desired temperature of the wedge. This typically took about 45 to 60 minutes. Once the temperature of the wedge shaped hot plate was stabilized, three type-K thermocouples with bead size of 0.38 mm were mounted along the centerline of the wedge at 6.4, 12.7 and 19.1 mm from the base (shown in Fig. 1 and labeled as 1, 2, and 3). These thermocouples allowed monitoring of the temperature of the coal dust in the wedge as a function of time. The wedge was then gently filled with a pre-measured amount of coal dust and the surface of the layer was evenly leveled with a flat iron ruler. In all the experiments, the wedge is

packed with a coal dust layer 25.4 mm thick (measured from the apex of the wedge) and 73.5 mm wide (in the direction perpendicular to the paper). The ends of the dust layer were blocked by 12.7 mm ( $\frac{1}{2}$ " ) thick insulations (Kaowool®) triangular piece as shown in Fig. 1. Tests were run until either the layer temperature reached a steady state for no less than 60 minutes or clear thermal runaway was observed. If thermal runaway did not occur at the pre-set plate temperature ( $T_p$ ), it was increased by 10°C until thermal runaway was observed. Once ignition was observed, the resolution between ignition and no ignition cases was fine tuned to within 5°C. Fresh coal samples were used for each test. To ensure repeatability in the temperatures recorded by the 3 thermocouples, each ignition experiment was then repeated at least four times. Figure 2 shows average temperatures recorded by three thermocouples for 90° wedge with the plate temperature set at 195°C. Deviations in transient temperature variations obtained from four different tests are represented by gray bands. It can be noted that the tests are consistent and produce temperature variations within  $\pm 7$  °C. Table 1 reports the average ignition times. Since the onset of ignition is not instantaneous, the ignition time is calculated by taking the average of the time instants where the temporal variation of temperature changes its slope before and after the rapid rise as shown in Fig. 3.

### 3. Results and Discussion

The temperatures recorded by the three thermocouples for the wedge shaped hot plates are shown in Fig. 4. Figure 4a shows the no-ignition scenario for 60° wedge, where the plates are maintained at 185 °C. When the temperature of the plates is increased by 5°C to 190 °C, the coal in the 60° wedge ignites and the *first ignition* is recorded by the top thermocouple. Only the top region ignites for this case, indicated by the temperature profile of the top thermocouple, which records a temperature 50 °C more than the hot plate temperature of 190 °C (Fig. 4c). For the 90° wedge, ignition occurs at 195 °C, which is 5 °C higher than the 60° case (Fig. 4d). This is because the rate of heat transfer from the hot plate to the symmetry plane is lower in the 90° wedge than in the 60° wedge. Unlike the acute-angle case, both top and middle thermocouples record rapid temperature rise indicating that both regions ignite almost simultaneously (around 60 minutes), as shown by the enlarged inset in Fig. 4d. The slopes of the temperature profiles before the onset of ignition are also different for the two wedges. For the 60° wedge, the temperature plateaus before the onset of ignition (Fig. 4c), while for the right-angled wedge, the temperatures continuously and gradually increase before the onset of ignition (Fig. 4d). The difference in ignition behavior between the two geometries and their implication to hazardous dust build up in industrial settings is discussed in the following sections.

### 3.1 Identification of Controlling Processes

There are three processes which control the ignition behavior in a wedge, namely, the heat transfer from the hot plate to the coal dust, the subsequent chemical heat release, and the heat transfer between different regions within the coal dust. Equation (1a) shows the general energy balance for spontaneous ignition [13], which can be applied to the wedge geometry in a cylindrical coordinate system ( $r$ - $\theta$ ) depicted in Fig. 5. The second term in the RHS of equation (1b) represents the heat flux from the hot-plate to any point within the coal dust layer acting along a normal  $n$  perpendicular to the plate (shown by 1'-1, 2'-2, and 3'-3 in Fig. 5). The heat flux from one region to another within the coal layer can be investigated in the radial direction (first term in RHS of equation 1b).

$$\nabla \cdot \vec{q} + \rho QA \exp\left(\frac{-E}{R_a T}\right) = \rho c \frac{\partial T}{\partial t}. \quad (1a)$$

$$\vec{q} = k \frac{\partial T}{\partial r} \hat{e}_r + k \frac{\partial T}{r \partial \theta} \hat{e}_\theta. \quad (1b)$$

In equations (1a) and (1b),  $QA$  and  $E$  are the pre-exponential factor and the activation energy,  $k$ ,  $\rho$ , and  $c$ , represent the thermal conductivity, density and specific heat of the coal dust, respectively, and  $\hat{e}_r$  and  $\hat{e}_\theta$  represent the unit vectors in  $r$  and  $\theta$  directions, respectively. The heat flux in  $\theta$ -direction can be written as,

$$k \frac{\partial T}{r \partial \theta} = k \frac{\partial T}{\partial n}. \quad (1c)$$

The second term in equation (1a) represents the chemical heat released per unit volume. Consistent with previous studies [8-10, 13] it is assumed that reactant consumption is negligible and the order of the reaction is zero. During all the tests, the coal dust is packed in the wedge using a mass equal to the volume of packing multiplied by its bulk density, so that the packed density and the bulk density are almost the same. As a result, the permeability in the packed dust layer is expected to be very small and it can be assumed that oxygen transport into the coal dust is negligible until the onset of ignition. It is possible that a post-ignition scenario that leads to a smoldering process, oxygen diffusion would come in to play [15]. However, this part of the problem is not analyzed.

The three processes controlling the ignition behavior are studied using a scaling type analysis using experimentally measured temperatures fitted into algebraic equations formed by the three terms in the left hand side of the governing equation (1a). The temporal variations thus obtained are then used to qualitatively analyze the strengths of the three processes at any time instant. The algebraic equations for the three terms are given as follows:

(a) Heat flux from the hot plate to a thermocouple location is calculated based on the difference in temperature between the two divided by the horizontal distance between them ( $n-n'$ ). This is given as follows:

$$k \frac{\partial T}{r \partial \theta} = k \frac{\partial T}{\partial n} = k \frac{T_p - T_n}{n - n'} \left( \frac{W}{m^2} \right); \quad n = 1, 2, 3. \quad (2)$$

(b) The heat transfer per unit area, between the lowermost to middle, and middle to top regions, are calculated based on the second term in equation (1) as follows:

$$\dot{q}''_{[n-(n+1)]} = k \frac{\partial T}{\partial r} = k \frac{T_n - T_{n+1}}{r_n - r_{n+1}} \left( \frac{W}{m^2} \right); \quad n = 1, 2, 3, \quad (3)$$

where a positive value of  $\dot{q}''_{[n-(n+1)]}$  denotes heat transfer in the upward direction.

(c) The third term in equation (1a) represents the volumetric source term given by:

$$\dot{q}'''_i = \rho Q A \exp \left( \frac{-E}{R_u T_i(t)} \right) \left( \frac{W}{m^3} \right); \quad i = 1, 2, 3. \quad (4)$$

The heat generation is calculated in  $W/m^3$  based on the temperature measured by the thermocouple at any time instant. To summarize, equations (2) and (3) represent the heat flux from the hot plate to a point and the heat dissipation between adjacent layers respectively. The heat release is determined per unit volume and is given by equation (4).

### 3.2 Relative Strengths of the Controlling Processes

The heat fluxes from the hot plate to all the thermocouples, evaluated by equation (2), are shown in Fig. 6, for 60° wedge (Fig. 6a) and 90° wedge (Fig. 6b). The vertical gray lines shown in Fig. 6 represent the onset of ignition or the ignition time (reported in Table 1). It is observed that just prior to ignition the heat flux received by the lowermost thermocouple is the highest irrespective of the wedge angle, due to its closeness to the hot plate. Correspondingly this thermocouple records the maximum temperature for both the wedges prior to ignition (Fig. 4). However, the lowermost thermocouple does not record ignition, which can be explained by analyzing the rate of heat release and heat dissipation.

Figure 7 shows temporal variation of heat release at any thermocouple position and the heat fluxes between points 1-2 and 2-3 calculated using the appropriate temperatures recorded by the thermocouples 1, 2, and 3. Only the time before ignition, which is important for the analysis, is considered. The trends of variations of these quantities would give an idea of their qualitative relative strengths at each point and at each time instant. This is analyzed for each wedge angle.

### *60° Wedge*

In spite of recording the highest temperature before ignition (around 59 min), Fig. 7a shows that the heat generated in the lowermost layer is the lowest, mainly due to the continuous heat dissipation from this layer to the middle layer as shown in Fig. 7b. Both the top and middle layers receive similar amounts of heat from the hot plate (Fig. 6a). However, the reason the top region always ignites first is due to the continuous positive heat transfer from the middle to top as shown by Fig. 7b (2-3). As a result, the temperature (Fig. 4c) and thus, the heat generation (Fig. 7a) in the top region, starts to increase around 48 minutes and eventually causes the top thermocouple to reach the ignition criterion.

### *90° Wedge*

For the 90° wedge, the overall heat release rates in all the regions are significantly higher compared to the 60° wedge (Figs. 7a and 7c) even though the hot plate temperatures are not significantly different between the two wedges. Both middle and top regions ignite (Fig. 4d) almost simultaneously (around 64 and 62 minutes, respectively). The heat release recorded by thermocouple 2 is also the maximum (Fig. 7c). The continuous positive heat transfer from the middle to top region (Fig. 7d) does not affect the heat release scenario in the middle region, rather it helps the top region to record sufficient heat release (Fig. 7c) to cause ignition. Therefore, due to monotonically increasing heat release in the middle region, that region reaches the ignition criterion and also favors the top region to reach the ignition criterion by providing good amount of heat flux.

The ignition behavior observed in the two wedge angle cases provides significant insight to hazardous conditions that can develop due to dust deposits trapped in corners. It is observed that in acute angle wedges the top layer ignites and as the angle increases, the ignition zone moves to inner layers. The results show that dust build up in acute angled wedges pose increased level of hazardous conditions since the high-temperature top layer can ignite flammable material in its vicinity.

### **3.3 Safety in Industrial Environments Exposed to Dust Layers**

The ASTM standard E 2021 and the European standard EN 50281-2-1(1999) are current test methodologies used in practice to estimate the minimum ignition temperature of fugitive dust layers. The minimum ignition temperature obtained from these tests represents the minimum temperature of a flat hot plate at which a dust layer ignites. These tests are phenomenally one-dimensional in nature. The mathematical model of this test has an explicit solution first developed by Thomas and Bowes [13]. Since there is no influence of geometry, for the flat plate case, all three regions (lowermost, middle and upper) of a dust layer ignite in this case. This has been confirmed with experimental data reported by Park et al. [10] for the same type of coal dust (Pittsburg Seam Coal). Experiments using the standard test apparatus

(flat plate equivalent to a  $180^\circ$  wedge) were also performed and showed that the minimum ignition temperature decreases nonlinearly with layer thickness as shown in Fig. 8, consistent with the thermal theory of ignition (Thomas and Bowes) as well as experimental data of Park et al. [10]. The curve in Fig. 8 delineates the no-ignition zone against the regions where a combination of plate temperature and layer thickness can sustain ignition.

At the onset of ignition, the net dissipative heat flux and volumetric heat generation can be coupled to form an effective length scale, which represents an effective thermal diffusion length scale, such that heat dissipation is balanced by the heat generation. This length scale can be used to determine the feasibility of ignition and for the standard test with flat dust layer heated at one end, it is equal to the thickness of the layer itself. The heat transfer processes in the case of a wedge is two dimensional in nature and hence difficult to resolve using a simple analytical model as in the case of a flat plate. However, an approximate thermal diffusion length scale similar to that in the flat plate case can be determined based on the distance of the thermocouple location from the hot plate, as shown in Fig. 5. That is, the distance between any thermocouple and the hot plate, as indicated in Fig. 5, will be equivalent to a coal layer thickness on a flat horizontal hot plate. Therefore corresponding to that thickness, a suitable ignition temperature, as given by the curve in Fig. 8, would be needed to initiate ignition at that layer. Several other combinations such as the ratio of volume to surface area of spheres, cylinders or trapezoidal shapes in the regions surrounding each thermocouple would also provide similar qualitative results.

Also shown in Fig. 8 is the temperatures recorded by all the three thermocouples at the time of ignition for both the wedges (reported in Table 2). It should be noted that the lowermost and middle thermocouples in the  $60^\circ$  wedge and the lowermost thermocouple in the  $90^\circ$  wedge fall in the no-ignition region when plotted against the effective length scale discussed above. The top thermocouple in the  $60^\circ$  wedge, and the middle and the top thermocouples in the  $90^\circ$  wedge reach the ignition region because of their increased effective lengths from the hot plate. The effective length scale can be determined by only using the geometric factors for different configurations, since this is based on the distance of a particular location from the hot plate. Since standard flat hot plate experimental data is available for most hazardous dusts, the approach presented in Fig. 8 can be useful in determining the ignition behavior of dust collected in several geometrical configurations.

### **3.3 Ignition at Elevated Plate Temperatures**

The influence of the controlling processes of heat transfer and energy generation on ignition characteristics of coal dust in a  $60^\circ$  and  $90^\circ$  wedges are further analyzed by increasing the temperature of the hot plates above the minimum ignition temperature (hot plates are maintained at  $20^\circ\text{C}$  and  $45^\circ\text{C}$

above the corresponding minimum ignition temperatures). The hot plate temperatures for 60° wedge are 210 °C (Fig. 9a) and 235 °C (Fig. 9c) and for the 90° wedge, the temperatures are 215 °C (Fig. 9b) and 240 °C (Fig. 9d). As the hot plate temperature is increased, the onset of ignition is seen to occur at an earlier time instant (Table 1), due to the increased availability of the amount of heat. Figure 9 shows that in both wedge geometries, temperature recorded by the top thermocouple decreases after the rapid increase. It is observed that this decrease in the temperature coincides with formation of cracks on the top surface, which facilitates the diffusion of cold ambient air into the top region. The cracks seem to influence the top region alone and the temperatures recorded by the middle and bottom do not decrease, instead reach steady values as shown in Fig. 9.

Figure 10 shows the temperatures recorded by the thermocouples in both the wedges at the time of ignition, along with the flat plate ignition temperature data. It can be observed that the minimum ignition temperature vs. layer thickness curve delineates the data for the cases with hot plate temperature higher than the corresponding minimum ignition temperatures of both wedges. Clearly, top and middle thermocouples in the 90° wedge record ignition at the hot plate temperature of 215°C (Fig. 10a) and only the top thermocouple records ignition for the 60° wedge at the hot plate temperature of 211°C. The same trend is observed in Fig. 10b, where the corresponding hot plate temperatures are 240°C and 235°C, respectively, for 60° and 90° wedges.

The maximum temperatures for three different plate temperatures conducted in this study are plotted in Fig. 11. The peak temperatures recorded in the 60° wedge are always lower than the 90° wedge. For the 60° wedge the peak temperature increases as plate temperature is increased. This is mainly due to an enhancement in heat generation with an increase in the hot plate temperature. For the 90° wedge, when the hot plate temperature is 45 °C more than the minimum ignition temperature, the maximum temperature recorded is only around 280 °C, that is, 10 °C less than the maximum temperature recorded in the case where the base temperature is 20 °C above the minimum ignition temperature.

Similar to Fig. 7, variations of heat released in a given region and heat conducted from one region to another is shown in Fig. 12 and Fig. 13, for cases where the plate temperatures are maintained at 20°C and 45°C, above the corresponding minimum ignition temperatures, respectively. The trends in the variations of these quantities for 60° wedge (Figs. 12a, 12b) and 90° wedge (Figs. 12c, 12d) are similar to their respective cases in Fig. 7. However, the amount of heat release has significantly increased in both wedges at higher plate temperature although the heat dissipation has not altered significantly. This explains the increase in the maximum temperature in the domain for both wedges. At still higher plate temperatures (45 °C above minimum ignition plate temperature) the trends in the variations of these quantities for 60° wedge (Figs. 13a, 13b) and 90° wedge (Figs. 13c, 13d) are different than the earlier cases presented in Figs. 7 and 12, especially for 90° wedge case. The heat release in the top region

increases significantly equalling that obtained in the middle region (Fig. 13c). This is due to the increased rate of heat dissipation from middle to top region (Fig. 13d). Therefore, at elevated temperatures heat generated is efficiently dissipated between regions resulting in a reduction in the maximum temperature in the case of the 90° wedge.

The results show that ignition behaviour at elevated temperatures shows different characteristics compared to ignition observed at the critical minimum ignition temperature. The heat dissipation between adjacent layers distributes the heat generated due to chemical reaction uniformly making it difficult suppress or extinguish such events from an industrial hazard perspective.

#### **4. Conclusions**

Ignition behavior of bituminous coal dust deposited in a 60° and 90° wedge shaped hot plates is experimentally studied. Interestingly, the dust around the apex of the wedge, which receives the maximum heat flux from the hot plates, never ignites. Instead, tests show that the top layer of coal dust records ignition in the case of 60° wedge and both the top and the middle regions record ignition in the case of 90° wedge. This unique behavior is examined by three parameters affecting the ignition, namely, the heat transfer from the hot plate to the coal dust, the subsequent chemical heat release and the heat transfer between different points within the coal dust. A thermal diffusion length scale is used to illustrate that the minimum ignition temperature increases as this length decreases. The influence of wedge geometry is also examined using this concept.

An increase in the hot plate temperature beyond the minimum ignition temperature affects the ignition characteristics (occurrence of ignition at an earlier time and higher value of maximum temperature within the coal dust) but the same trend of ignition location is maintained. The ignition behavior observed in the two wedge angle cases provides significant insight to hazardous conditions that can develop due to dust deposits trapped in corners. The results show that dust build up in acute angled wedges pose increased level of hazardous conditions since the high-temperature top layer can ignite flammable material in its vicinity.

#### **Acknowledgements**

The authors would like to thank the National Science Foundation award #0846764 for funding this work under the American Reinvestment and Recovery Act of 2009. The assistance from students John Desrosier, and Alexander Andrews for construction of the wedge hot plate apparatus as part of a final year undergraduate project and Haejun Park for the flat hot plate apparatus is graciously acknowledged. Finally the authors would like to thank Richard Winschel (CONSOL Energy) and Evan Granite (DOE-NETL) for providing free coal dust for testing.

## References

- [1] R. K. Eckhoff, Dust explosions in the process industries. 3 ed., Boston: Gulf Professional Publishing/ Elsevier, 2003.
- [2] J. Gummer and G. A. Lunn, J. Loss Prevent. Proc. 16 (2003), 27-32.
- [3] W. Bartknecht, Explosions: Course, prevention, protection., Berlin: Springer-Verlag New York, 1989.
- [4] W. E. Baker and M. J. Tang, Gas, dust, and hybrid explosions. Elsevier Publishing Company, 1991.
- [5] Y. Miron, C. P. Lazzara. Fire Mater. 12 (1988) 115-126.
- [6] ASTM. Standard test method for hot surface ignition temperature of dust layers. ASTM E 2021. (2003).
- [7] Electrical apparatus for use in the presence of combustible dust—part 2-1: test methods—methods of determining minimum ignition temperatures EN 50281-2-1 (1999).
- [8] P. C. Bowes, S. E. Townshend. Brit. J Appl. Phys. 13 (1962) 105-114.
- [9] P. D. Reddy, P. R. Amyotte, M. J. Pegg, Combust. Flame (1998) 41-53.
- [10] H. Park, A. Rangwala, N. Dembsey, J. Hazard. Mater. 168 (2009) 145-155.
- [11] H. M. Kim and C. C. Hwang, Combust. Flame 105 (1996) 471-485.
- [12] Z. Dyduch, B Majcher, J. Loss Prevent. Proc. 19 (2006) 233-237.
- [13] P. H. Thomas, P. C. Bowes, T. Faraday Soc. (1961) 2007-2017.
- [14] T. Boddington, P. Gray, D. I. Harvey, Philos. T. Roy. Soc. S-A. (1971) 467-506.
- [15] T. J. Ohlemiller, Prog. Energy Combust. Sci. 13 (1985) 277-310.

### List of Tables:

Table 1: Ignition time data in minutes

Table 2: Temperatures of the thermocouples at the time of ignition for both wedges

### List of Figures

Figure 1: (a) Wedge shaped hot plate experimental setup (isometric view). (b) Cross-section of wedge along the plane of symmetry. All dimensions are in mm.

Figure 2: Average temperature variation with time, obtained from four tests in 90° wedge with the plate temperature at 195 °C; grey bands indicate the deviations in the measured values from different tests. Horizontal grey lines indicate hot plates temperature ( $T_p$ ) and the temperature 50 °C more than  $T_p$ .

Figure 3: Ignition time determined by taking the average of the time instants where the transient temperature curve changes its slope before and after a rapid rise.

Figure 4: Temporal variation of temperature recorded at three locations; bottom (6.4 mm from the wedge apex), middle (12.7 mm from the apex) and top (19.1 mm from the apex) for (a, c) 60° wedge and (b, d) 90° wedge; temperature of the hot plates 185 °C (a), 190 °C (b, c) and 195 °C (d).

Figure 5: Cylindrical (r- $\theta$ ) coordinate system for a half-wedge configuration; n is the dimensional angular distance

Figure 6: Temporal variations of the temperature gradients normal to the hot plate in the direction of a normal vector connecting the hot plate and a thermocouple for (a) 60° wedge (hot plates maintained at 190°C) and (b) 90° wedge (hot plates maintained at 195°C), for all the three thermocouples.

Figure 7: Temporal variations of heat release (a, c) in the volume surrounding each thermocouple and heat conducted between regions 1 - 2 and between 2 - 3 (b, d), for 60° (a, b) and 90° (c, d) wedges, until ignition

Figure 8: Present experimental data of flat plate ignition studies (+) along with the data from a similar study by Park et al. [10] (x), and the temperature of thermocouples 1, 2 and 3 recorded at the time of ignition for both 60° and 90° wedges

Figure 9: Time histories of temperatures recorded by three thermocouples inside the dust layer when the hot plates are maintained at 20 °C above the minimum ignition temperature (a, b) and at 45 °C above the minimum ignition temperature (c, d) for 60 ° wedge (a, c) and 90° wedge (b, d)

Figure 10: Present experimental data of flat plate ignition studies (+) along with the data from a similar study by Park et al. [10] (x), and the temperature of thermocouples 1, 2 and 3 recorded at the time of ignition for both 60° and 90° wedges when the hot plate is at higher temperature than the corresponding minimum ignition temperatures

Figure 11: Maximum temperature reached inside the domain as a function of hot plate temperatures for 60° and 90° wedges

Figure 12: Temporal variations of heat release (a, c) and heat conducted (b, d), until ignition, in 60° (a, b) and 90° (c, d) wedges, when hot plates are maintained at 20 °C more than minimum ignition temperature

Figure 13: Temporal variation of heat release (a, c) and heat conducted (b, d), until ignition, in 60° (a, b) and 90° (c, d) wedges, when hot plates are maintained at 45 °C more than minimum ignition temperature.

**Table 1: Ignition time data in minutes**

$T_p$	60° Wedge		$T_p$	90° Wedge	
	TC3			TC2	TC3
190 °C	59		195 °C	64	62
210 °C	38		215 °C	46	43
235 °C	29		240 °C	34	32

Table 2: Temperatures of the thermocouples at the time of ignition for both wedges

Thermocouple	Temperature °C	
	60° wedge	90° wedge
1	177	203
2	199	240
3	240	245

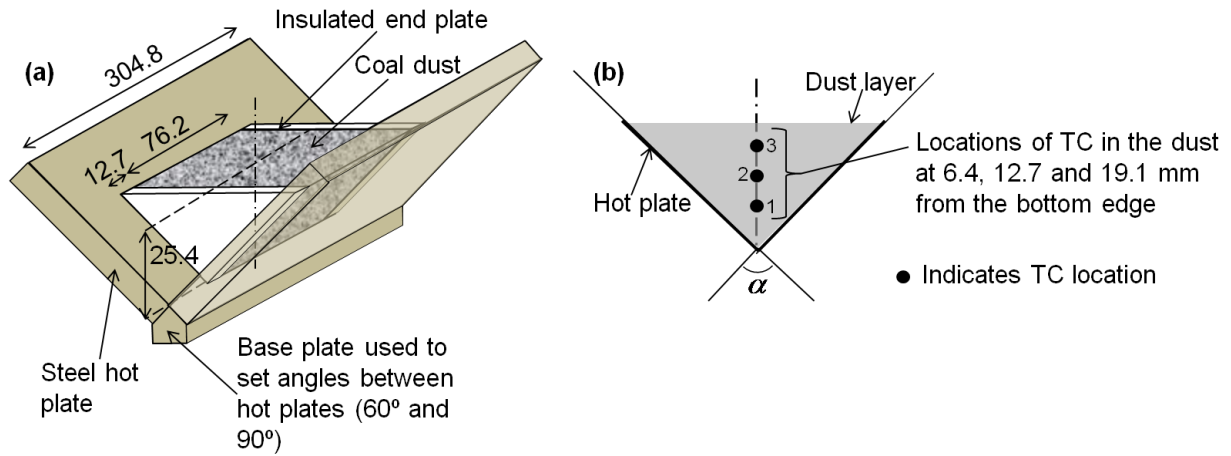


Figure 1: (a) Wedge shaped hot plate experimental setup (isometric view). (b) Cross-section of wedge along the plane of symmetry. All dimensions are in mm.

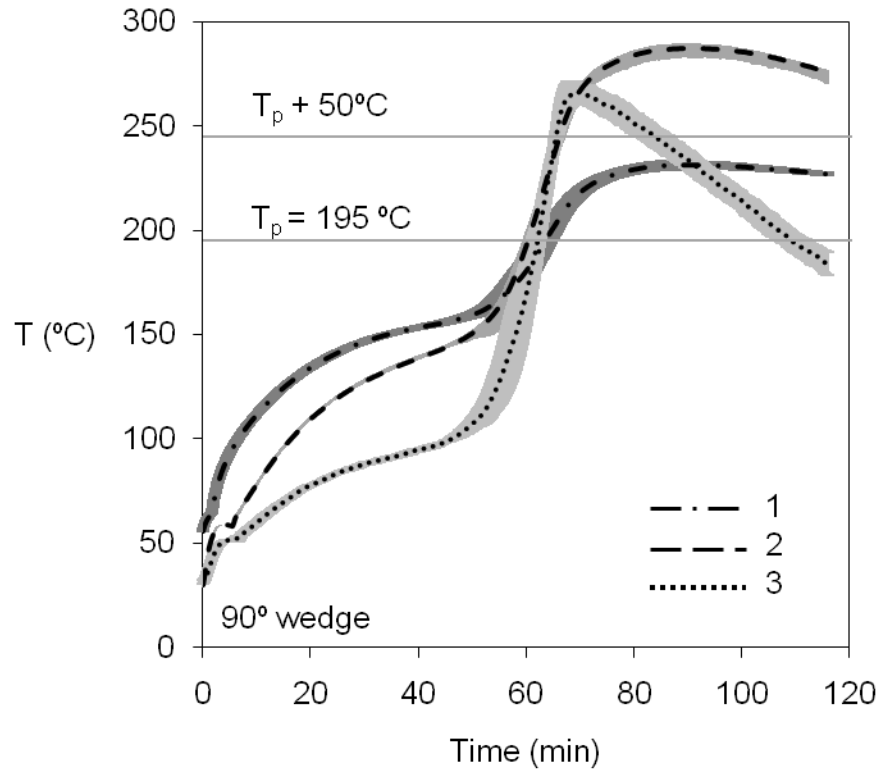


Figure 2: Average temperature variation with time, obtained from four tests in 90° wedge with the plate temperature at 195 °C; grey bands indicate the deviations in the measured values from different tests. Horizontal grey lines indicate hot plates temperature ( $T_p$ ) and the temperature 50 °C more than  $T_p$ .

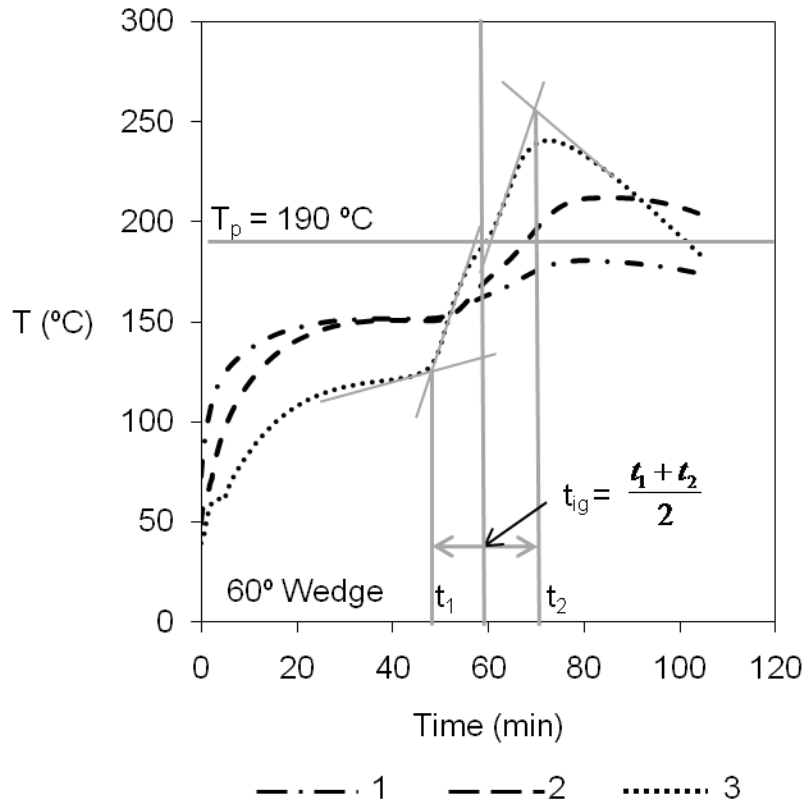


Figure 3: Ignition time determined by taking the average of the time instants where the transient temperature curve changes its slope before and after a rapid rise.

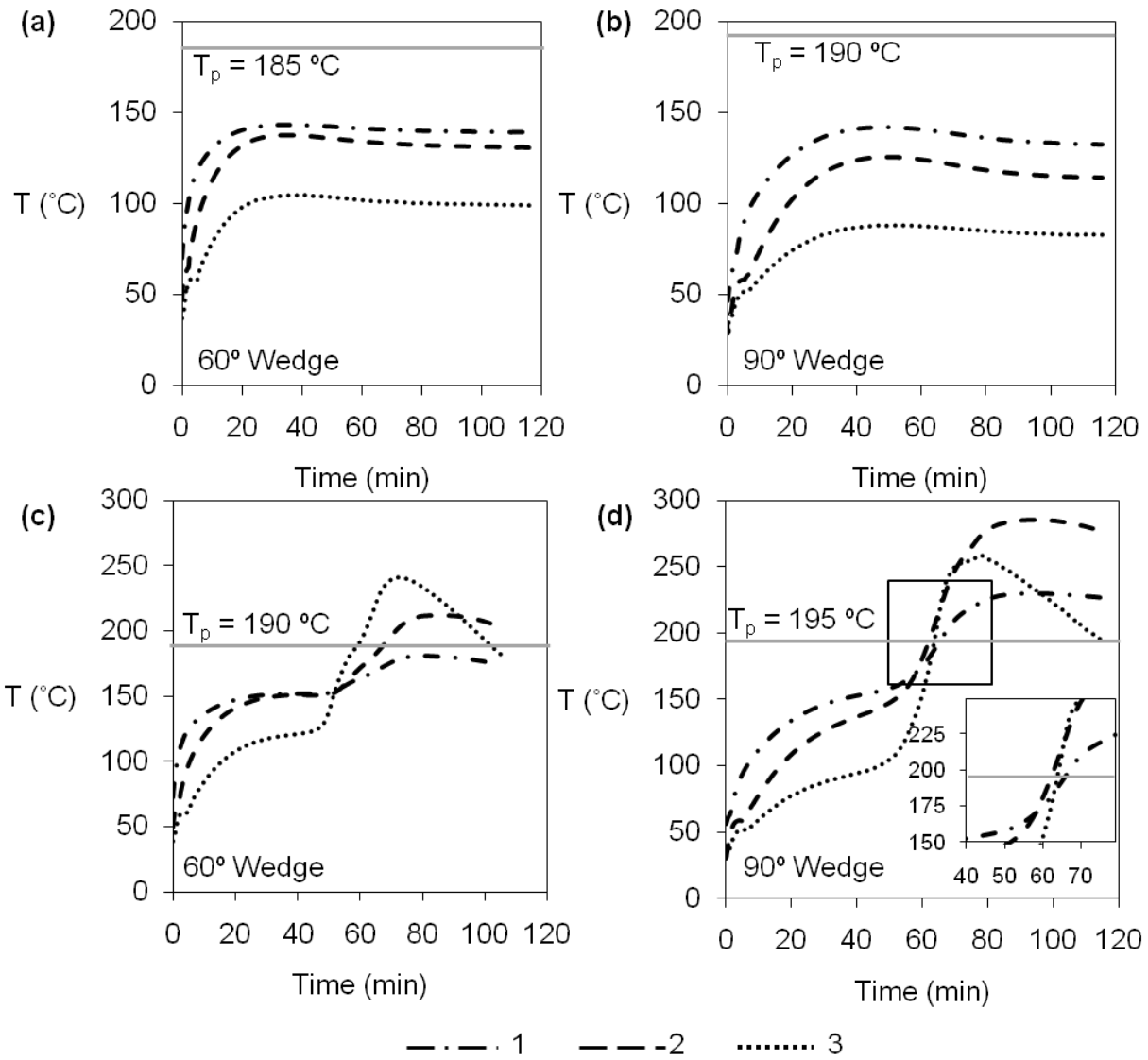


Figure 4: Temporal variation of temperature recorded at three locations; bottom (6.4 mm from the wedge apex), middle (12.7 mm from the apex) and top (19.1 mm from the apex) for (a, c) 60° wedge and (b, d) 90° wedge; temperature of the hot plates 185 °C (a), 190 °C (b, c) and 195 °C (d).

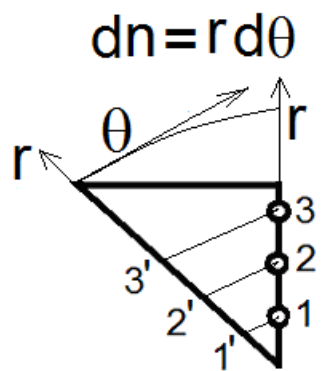


Figure 5: Cylindrical ( $r$ - $\theta$ ) coordinate system for a half-wedge configuration;  $n$  is the dimensional angular distance

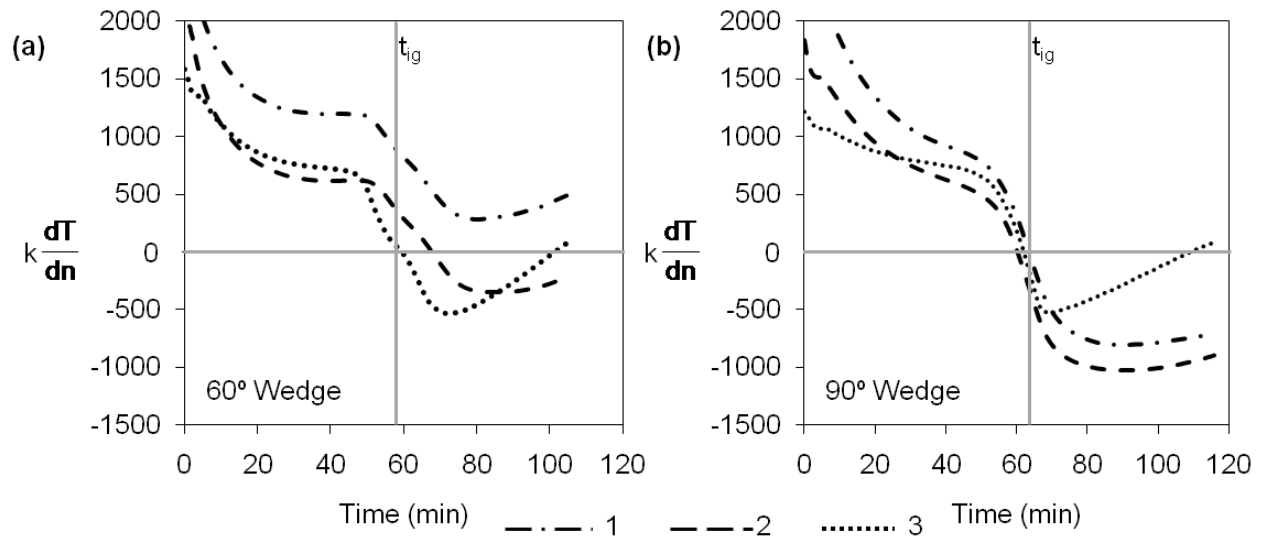


Figure 6: Temporal variations of the temperature gradients normal to the hot plate in the direction of a normal vector connecting the hot plate and a thermocouple for (a) 60° wedge (hot plates maintained at 190°C) and (b) 90° wedge (hot plates maintained at 195°C), for all the three thermocouples

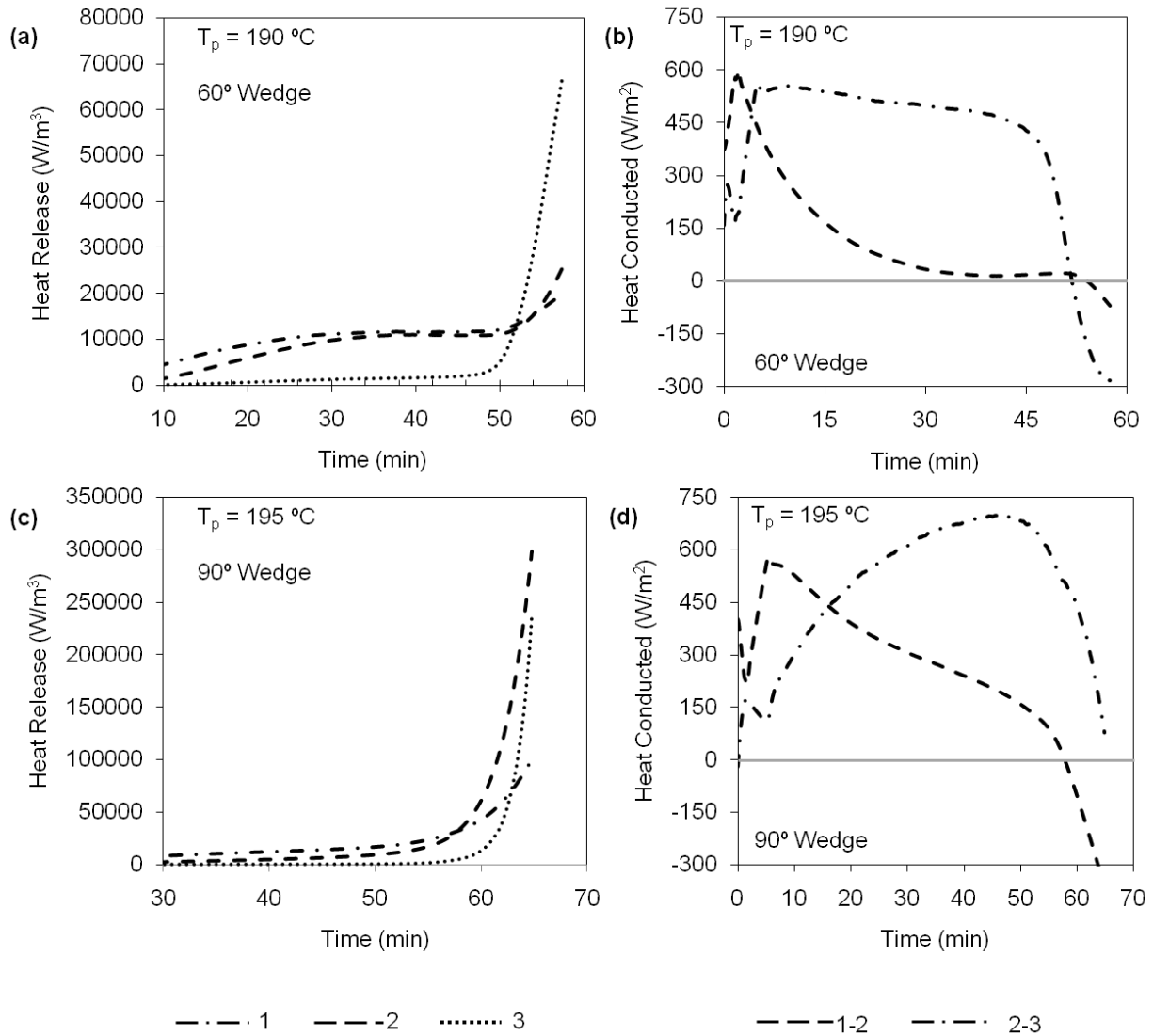


Figure 7: Temporal variations of heat release (a, c) in the volume surrounding each thermocouple and heat conducted between regions 1 - 2 and between 2 - 3 (b, d), for 60° (a, b) and 90° (c, d) wedges, until ignition

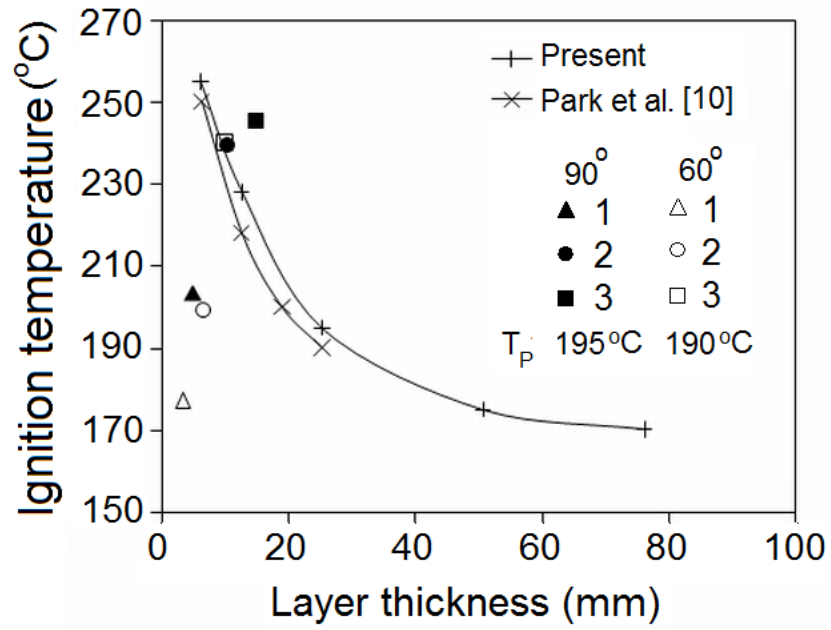


Figure 8: Present experimental data of flat plate ignition studies (+) along with the data from a similar study by Park et al. [10] (x), and the temperature of thermocouples 1, 2 and 3 recorded at the time of ignition for both 60° and 90° wedges

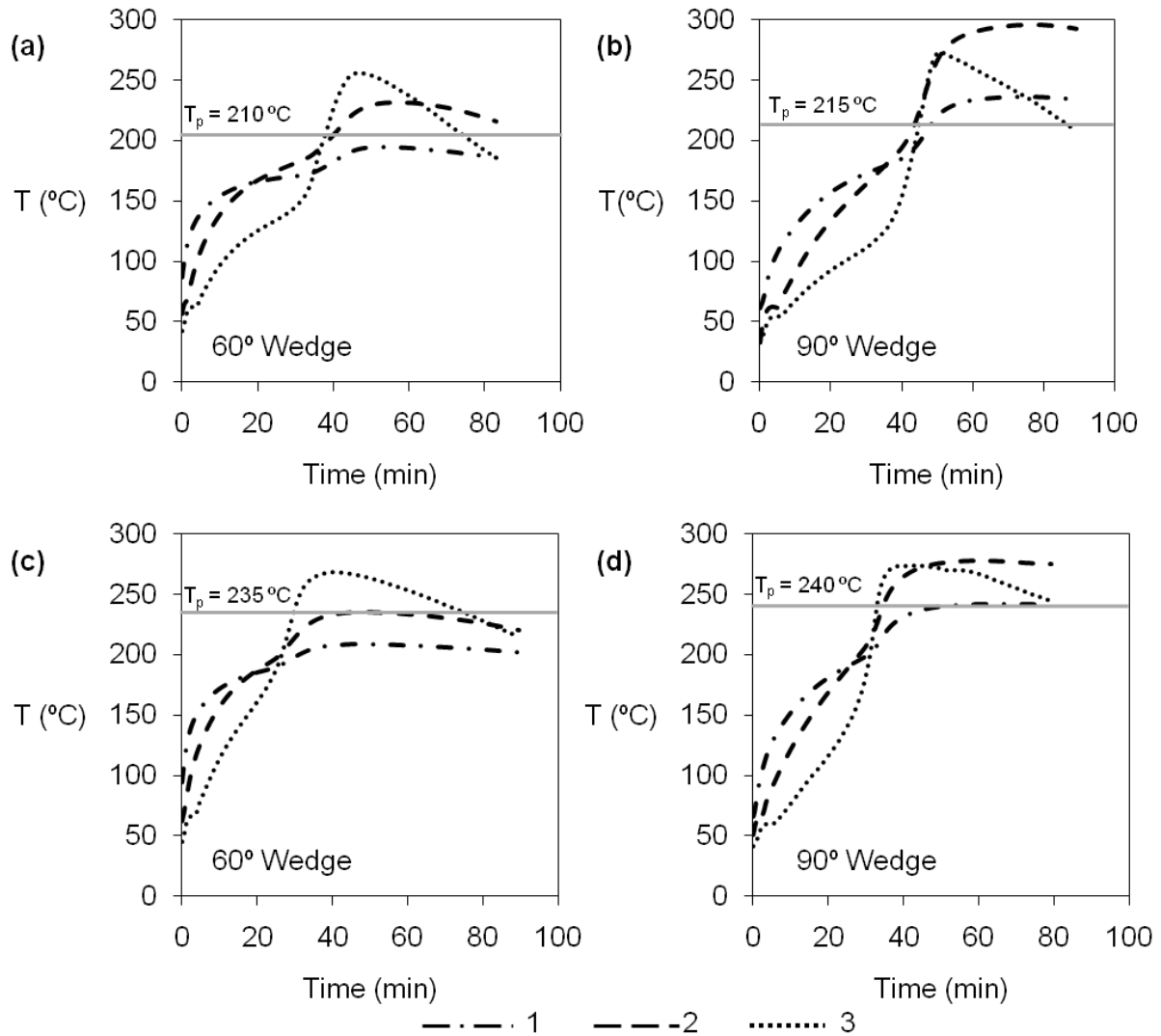


Figure 9: Time histories of temperatures recorded by three thermocouples inside the dust layer when the hot plates are maintained at  $20^{\circ}\text{C}$  above the minimum ignition temperature (a, b) and at  $45^{\circ}\text{C}$  above the minimum ignition temperature (c, d) for  $60^{\circ}$  wedge (a, c) and  $90^{\circ}$  wedge (b, d)

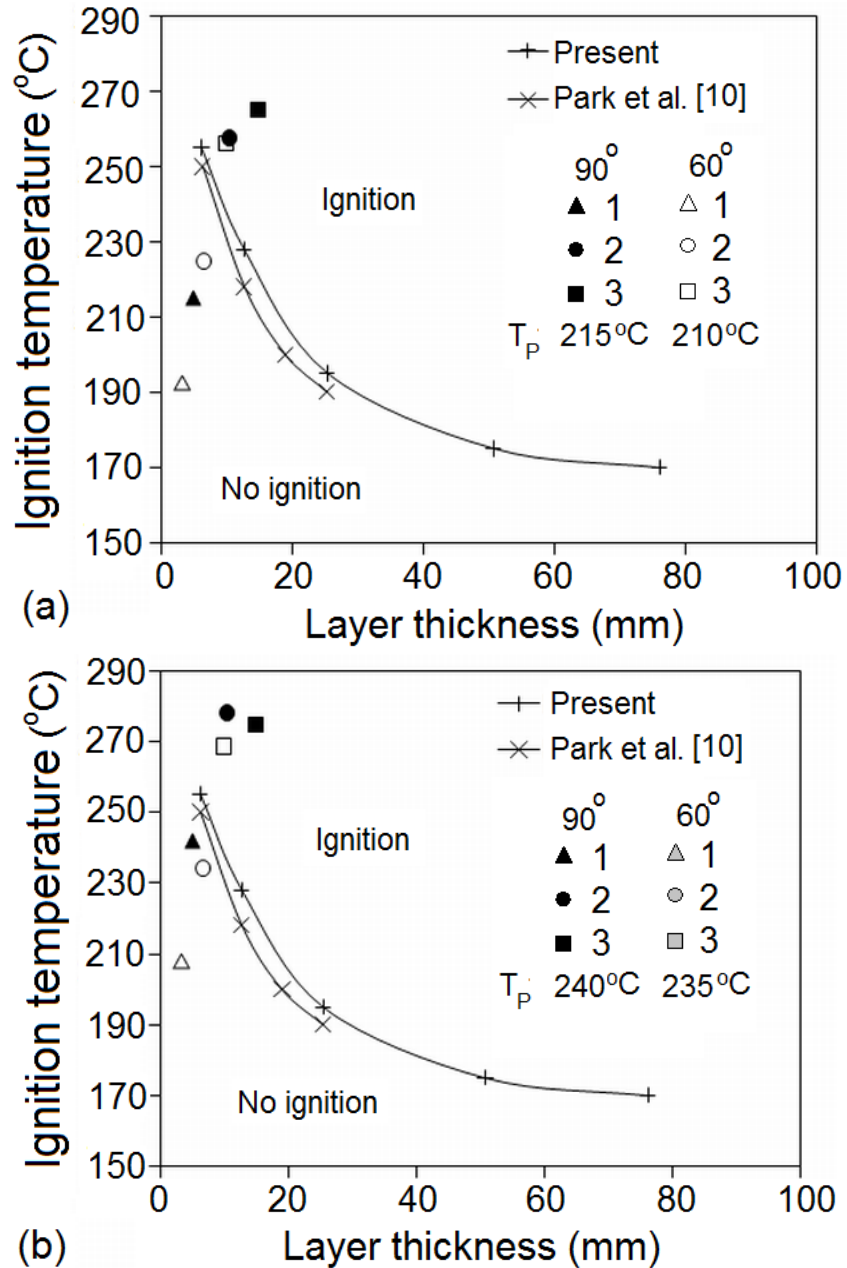


Figure 10: Present experimental data of flat plate ignition studies (+) along with the data from a similar study by Park et al. [10] (x), and the temperature of thermocouples 1, 2 and 3 recorded at the time of ignition for both 60° and 90° wedges when the hot plate is at higher temperature than the corresponding minimum ignition temperatures

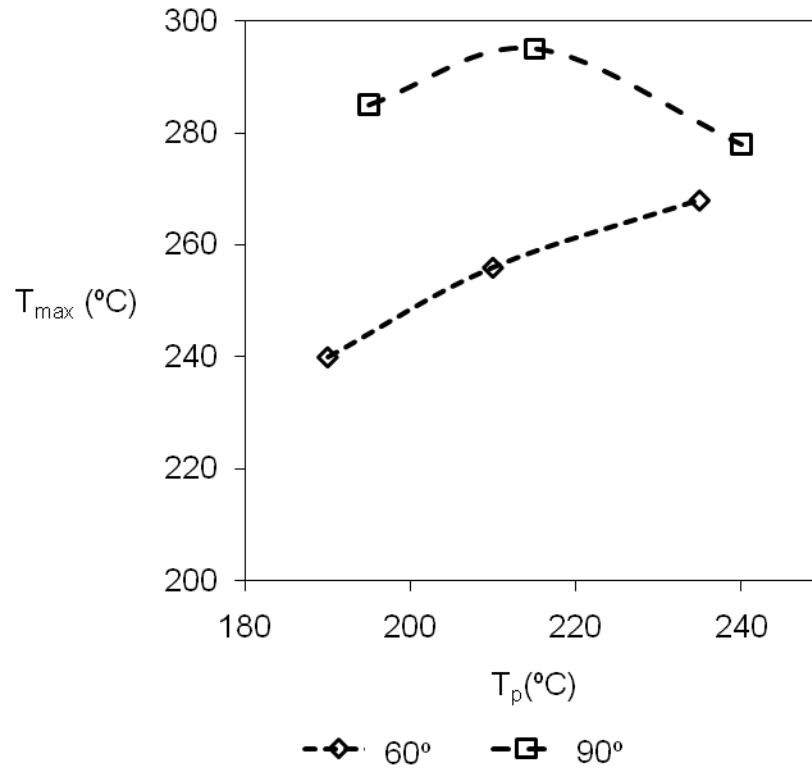


Figure 11: Maximum temperature reached inside the domain as a function of hot plate/base temperatures for 60° and 90° wedges

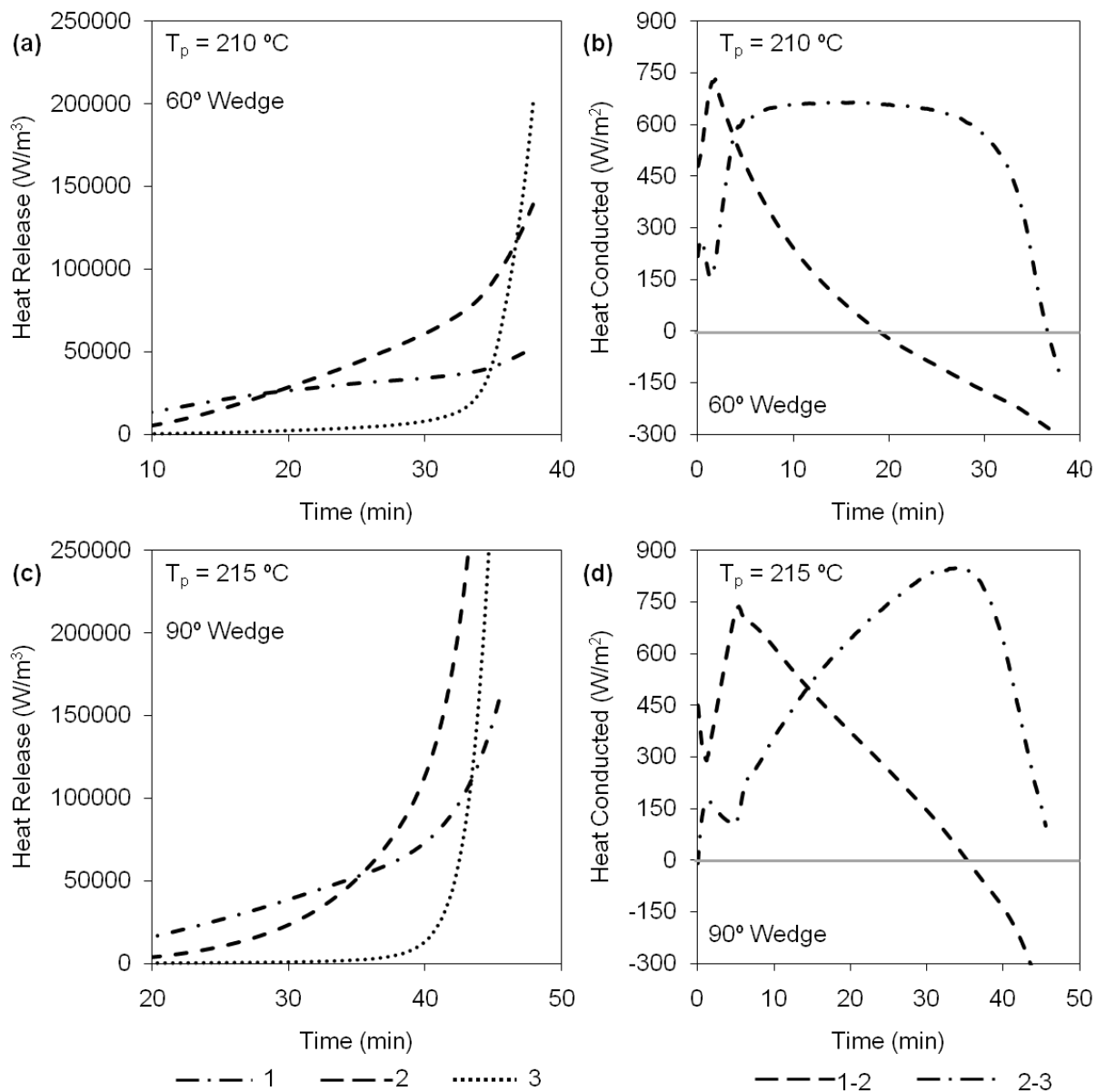


Figure 12: Temporal variation of heat release (a, c) and heat conducted (b, d), until ignition, in 60° (a, b) and 90° (c, d) wedges, when hot plates are maintained at 20 °C more than minimum ignition temperature

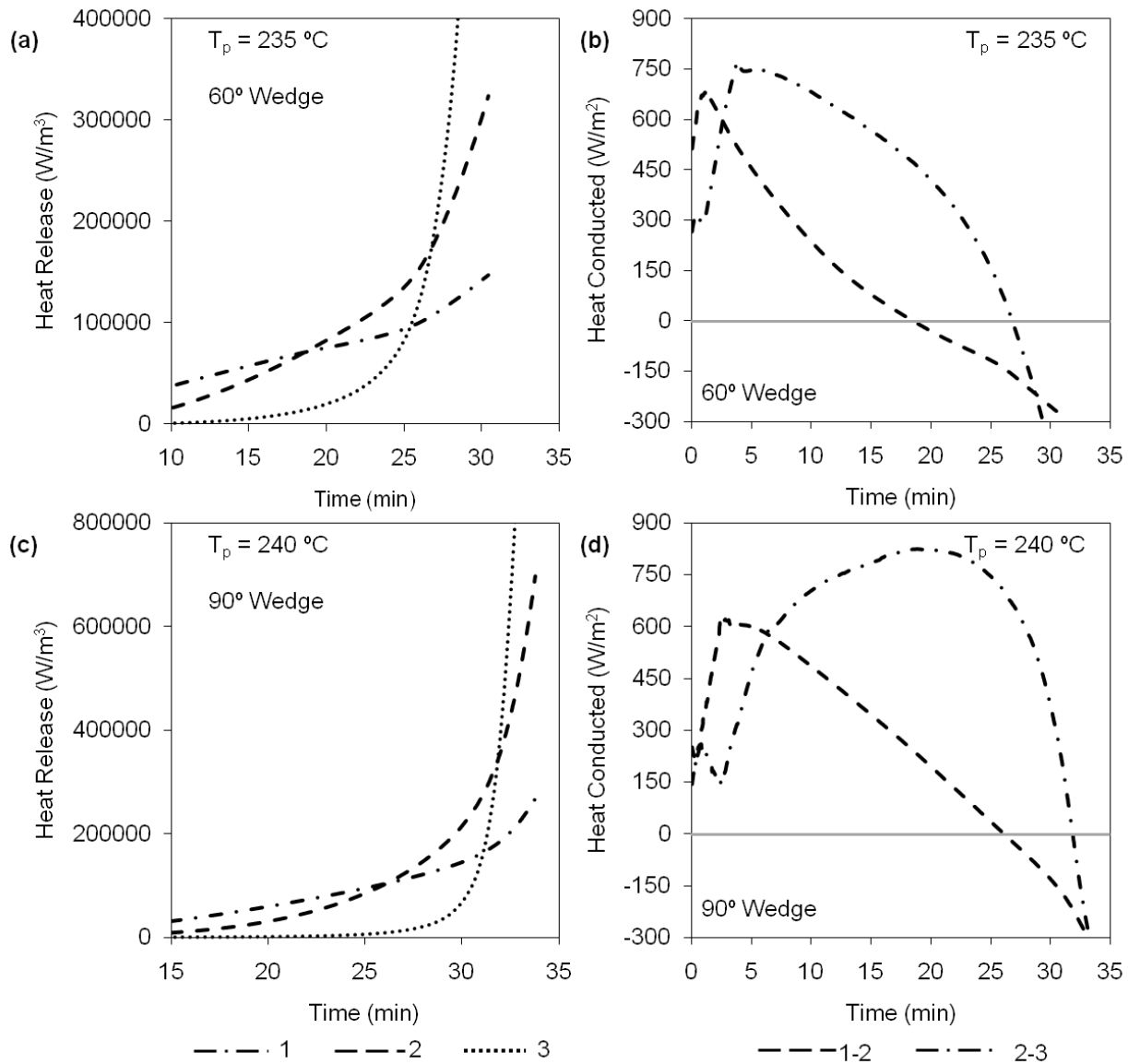


Figure 13: Temporal variation of heat release (a, c) and heat conducted (b, d), until ignition, in  $60^\circ$  (a, b) and  $90^\circ$  (c, d) wedges, when hot plates are maintained at  $45^\circ C$  more than minimum ignition temperature